

Glycogen Synthase Kinase 3 α -Specific Regulation of Murine Hepatic Glycogen Metabolism

Katrina MacAulay,^{1,2} Bradley W. Doble,^{1,2,3} Satish Patel,¹ Tanya Hansotia,¹ Elaine M. Sinclair,¹ Daniel J. Drucker,¹ Andras Nagy,¹ and James R. Woodgett^{1,*}

¹Samuel Lunenfeld Research Institute, Mount Sinai Hospital, Toronto, ON M5G 1X5, Canada

²These authors contributed equally to this work.

³Present address: McMaster Stem Cell and Cancer Research Institute, McMaster University, Hamilton, ON L8N 3Z5, Canada.

*Correspondence: woodgett@mshri.on.ca

DOI 10.1016/j.cmet.2007.08.013

SUMMARY

Glycogen synthase kinase 3 comprises two isoforms (GSK-3 α and GSK-3 β) that are implicated in type II diabetes, neurodegeneration, and cancer. GSK-3 activity is elevated in human and rodent models of diabetes, and various GSK-3 inhibitors improve glucose tolerance and insulin sensitivity in rodent models of obesity and diabetes. Here, we report the generation of mice lacking GSK-3 α . Unlike GSK-3 β mutants, which die before birth, GSK-3 α knockout (GSK-3 α KO) animals are viable but display enhanced glucose and insulin sensitivity accompanied by reduced fat mass. Fasted and glucose-stimulated hepatic glycogen content was enhanced in GSK-3 α KO mice, whereas muscle glycogen was unaltered. Insulin-stimulated protein kinase B (PKB/Akt) and GSK-3 β phosphorylation was higher in GSK-3 α KO livers compared to wild-type littermates, and IRS-1 expression was markedly increased. We conclude that GSK-3 isoforms exhibit tissue-specific physiological functions and that GSK-3 α KO mice are insulin sensitive, reinforcing the potential of GSK-3 as a therapeutic target for type II diabetes.

INTRODUCTION

Glycogen synthase kinase 3 (GSK-3) is a serine/threonine kinase first identified as one of the primary regulators of glycogen synthase (GS) (Embi et al., 1980). GSK-3 exists as two ubiquitously expressed homologs, GSK-3 α (51 kDa) and GSK-3 β (46 kDa), which share 98% sequence similarity in their catalytic domains but differ in their N- and C-terminal regions (Woodgett, 1990). GSK-3 is constitutively active in unstimulated cells and is inactivated by a variety of cellular stimuli. The best documented signaling pathway resulting in GSK-3 inactivation is triggered by insulin, which initiates a cascade of events that activate protein kinase B/Akt (PKB/Akt), which in turn

phosphorylates a key serine residue located near the N terminus of GSK-3 (Ser21 of GSK-3 α and Ser9 of GSK-3 β), resulting in inactivation of GSK-3 (Frame et al., 2001). GSK-3 phosphorylates four of nine GS regulatory serine residues (Ser641, Ser645, Ser649, and Ser653), which play a critical role in inhibiting GS activity and hence glycogen synthesis (Roach, 2002).

Insulin resistance is key in the pathogenesis of obesity and type II diabetes and is characterized by the failure of insulin-sensitive tissues to efficiently absorb and store glucose in response to insulin (Kaidanovich and Eldar-Finkelman, 2002). Since GSK-3 is normally active, its inactivation by insulin is considered essential for a normal insulin catabolic response. Numerous studies have implicated dysregulation of GSK-3 in the pathogenesis of insulin resistance and type II diabetes. Elevated GSK-3 activity and expression have been observed in obese and diabetic humans and rodents (Eldar-Finkelman et al., 1999; Nikouline et al., 2000) and in the adipose tissue of high-fat-fed mice (Eldar-Finkelman et al., 1999). Recent studies have also demonstrated that inhibition of GSK-3 using small-molecule or peptide inhibitors improves insulin action and glucose homeostasis in rodent models (Dokken et al., 2005; Kaidanovich-Beilin and Eldar-Finkelman, 2006).

The majority of prior research has focused on the β isoform of GSK-3, while relatively little is known about GSK-3 α . Here, we have generated GSK-3 α knockout (GSK-3 α KO) mice, characterization of which shows that each isoform displays unique tissue-specific physiological functions. Loss of GSK-3 α results in not only improved glucose tolerance in response to a glucose load but also, strikingly, elevated hepatic glycogen storage and insulin sensitivity.

RESULTS

Generation of GSK-3 α KO Mice

Conditional GSK-3 α KO mice were generated by introducing LoxP sites flanking exon 2 of the GSK-3 α gene through homologous recombination (Figure 1A; described previously in Doble et al. [2007]). Germline deletion of GSK-3 α exon 2 was accomplished by crossing the heterozygous conditional KO mice with a pCAGGS (chicken β -actin) Cre deleter mouse strain. Mating of Cre-deleted

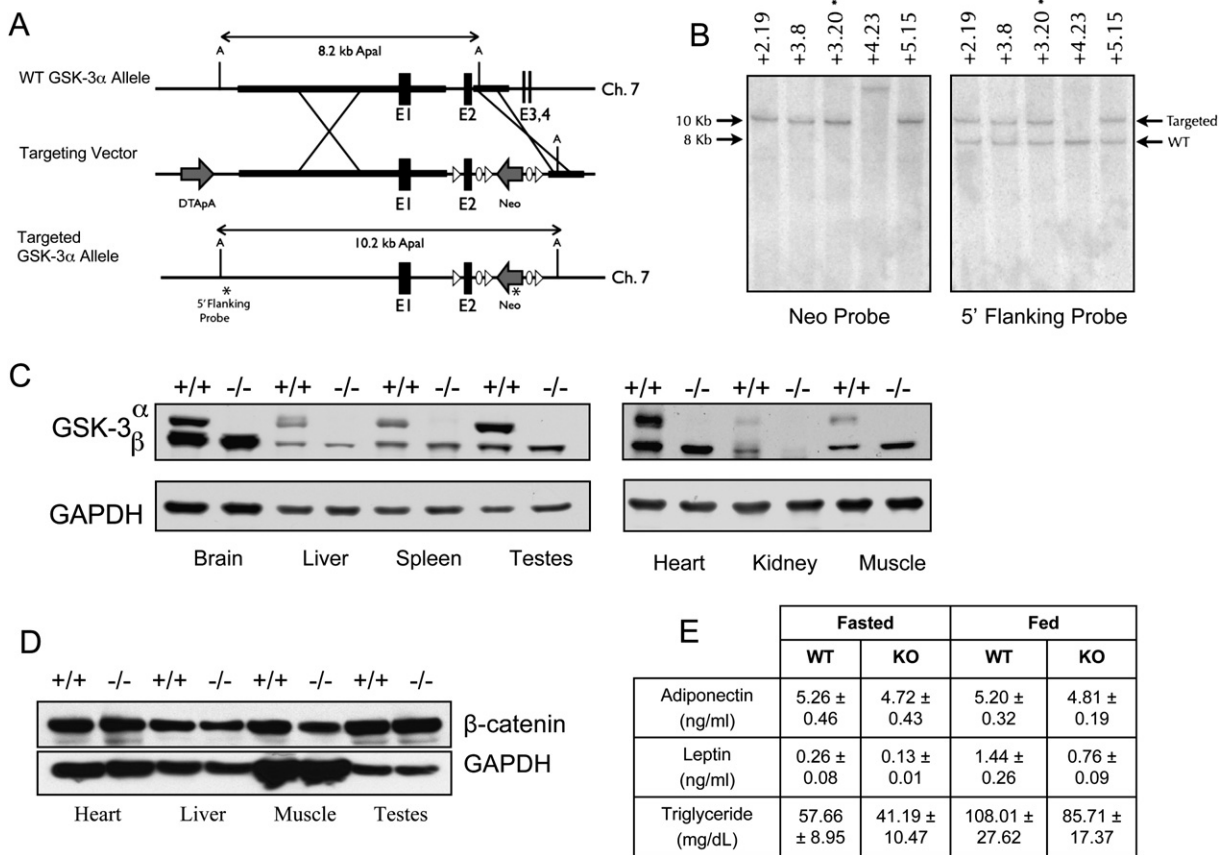


Figure 1. Targeting Strategy, Protein Expression, and Hormone/Triglyceride Levels of GSK-3 α KO Mice

(A) Proper homologous recombination between the GSK-3 α locus and the targeting vector results in the replacement of exon 2 (E2) with a LoxP-flanked exon 2 and a neomycin resistance cassette (Neo) flanked by FRT recombination sites. A = Apal sites; triangles = LoxP sites; ovals = FRT sites, DTApA = diphtheria toxin negative selection cassette; asterisks = Southern blot probe hybridization sites; bolded line segments = "arms" of homology.

(B) Southern blot analysis of five independent G418-resistant ES cell clones. Genomic DNA was digested with Apal and analyzed with the probes indicated in (A). Four of the five clones analyzed had expected band patterns.

(C) The indicated tissue lysate (20 μ g protein) was resolved by SDS-PAGE and immunoblotted with antibodies against GSK-3 α / β . Loading was monitored using antibodies to GAPDH. Blots are representative of three separate experiments.

(D) Heart, liver, muscle, and testes from 8-week-old GSK-3 α KO animals (-/-) and WT littermate controls (+/+) were extracted and lysed as described in *Experimental Procedures*, and proteins were resolved by SDS-PAGE. Proteins were detected by immunoblotting with antibodies against β -catenin.

(E) Adiponectin, leptin, and triglyceride concentrations were determined in 8-week-old male GSK-3 α KO animals and WT littermate controls under fasted and fed conditions. Values are mean \pm SEM from at least five separate animals.

GSK-3 α heterozygous animals generated GSK-3 α KO, heterozygous, and wild-type (WT) littermate control mice. GSK-3 α KO mice were both viable and fertile and displayed body mass similar to WT littermates (see *Figure S1A* in the *Supplemental Data* available with this article online).

Antibodies specific for GSK-3 α and β were used to demonstrate loss of GSK-3 α expression in all tissues tested (*Figure 1C*). Analysis of β -catenin protein levels demonstrated that inactivation of GSK-3 α does not result in β -catenin stabilization (*Figure 1D*). Analysis of plasma adiponectin and triglyceride concentrations revealed no significant differences between GSK-3 α KO and WT animals under fasted or fed conditions (*Figure 1E*). Plasma leptin concentrations were found to be slightly, although not significantly, lower in GSK-3 α KO animals under fasted

conditions. However, fed leptin levels were significantly lower in KO mice compared to WT control animals. Absolute food consumption over a 24 hr period was comparable between the two animal groups (*Figure S1B*).

GSK-3 α KO Mice Exhibit Improved Glucose Clearance

To test whether global loss of GSK-3 α resulted in improved glucose and insulin sensitivity, we performed glucose and insulin tolerance tests. GSK-3 α KO mice exhibited significant glycemic excursion after intraperitoneal (i.p.) glucose administration (*Figure 2A*). The improved glucose tolerance could be attributed to enhanced insulin secretion and/or improved insulin sensitivity. Fasted and fed plasma insulin concentrations were found to be similar in WT and GSK-3 α KO mice (0.12 \pm 0.01 ng/ml versus 0.11 \pm 0.01 ng/ml

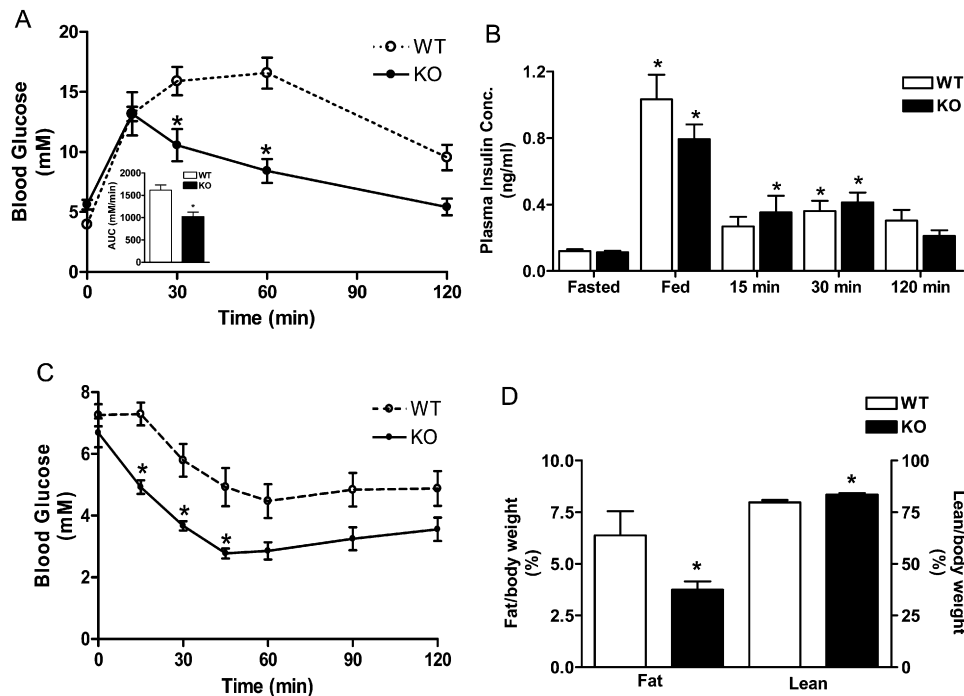


Figure 2. Glucose Tolerance, Insulin Sensitivity, Plasma Insulin Concentration, and Body Mass in GSK-3 α KO and WT Mice

(A) Blood glucose concentration in 8-week-old male GSK-3 α KO animals (●) and WT littermates (○) was measured at the indicated times following administration of 2 mg/g glucose by i.p. injection. Inset depicts the area under the curve (AUC) for WT (white bars) and KO (black bars) animals. $n \geq 12$ animals; * $p < 0.001$ versus WT. In this and all other figures, error bars represent the standard error of the mean.

(B) Plasma insulin concentration was determined in 8-week-old male GSK-3 α KO animals (black bars) and WT littermates (white bars) under fasted and fed conditions and 15, 30, and 120 min following an i.p. injection of glucose. $n = 8$ animals; * $p < 0.05$ versus the respective fasted control.

(C) Insulin tolerance was determined by measuring blood glucose concentration in 8-week-old male GSK-3 α KO animals (●) and WT littermates (○) at the indicated times following i.p. injection of 1 mU/g insulin as described in [Experimental Procedures](#). $n \geq 12$ animals; * $p < 0.001$ versus WT for 15 min; * $p < 0.01$ versus WT for 30 min and 45 min.

(D) Total body fat and lean mass normalized to body weight in GSK-3 α KO (black bars) and WT littermate control (white bars) mice. $n = 6$ animals; * $p < 0.05$ versus WT.

in the fasted state, respectively; 1.03 ± 0.15 ng/ml versus 0.79 ± 0.09 ng/ml in the fed state, respectively; [Figure 2B](#)). Furthermore, glucose-stimulated plasma insulin levels from GSK-3 α KO animals were comparable to those observed in WT animals.

To assess whether GSK-3 α inactivation affects insulin sensitivity, we carried out insulin tolerance tests in WT and KO mice. GSK-3 α KO animals showed enhanced ability to clear blood glucose compared to their WT counterparts ([Figure 2C](#)). Enhanced glucose tolerance and insulin sensitivity were also observed in GSK-3 α KO animals at 16, 24, and 32 weeks of age (data not shown). GSK-3 α KO animals exhibited a significant reduction in total body fat mass compared to WT animals ([Figure 2D](#)), and total body lean mass was significantly higher in GSK-3 α KO animals compared to WT animals.

Glucose Transport Is Not Increased in Muscle or Liver of GSK-3 α KO Mice

Immunoblot analysis of total cell membrane preparations from skeletal muscle revealed no differences in the levels

of GLUT1 and GLUT4 protein between WT and GSK-3 α KO mice ([Figure S2A](#)). Consistent with these observations, loss of GSK-3 α had no effect on basal (2.12 ± 0.37 μ mol/mg/hr WT versus 2.24 ± 0.20 μ mol/mg/hr KO) or insulin-stimulated glucose transport (5.77 ± 0.30 μ mol/mg/hr WT versus 5.30 ± 0.44 μ mol/mg/hr KO) in isolated soleus ([Figure S2C](#)) and extensor digitorum longus muscle (data not shown). Analysis of the glucose-dependent liver glucose transporter GLUT2 showed comparable GLUT2 protein levels in liver membranes from GSK-3 α KO and WT animals ([Figure S2B](#)).

Effects of Insulin and Glucose on Insulin Signaling Molecules

As GSK-3 is a key component of the insulin signal transduction pathway, we assessed the impact of GSK-3 α deletion on several molecules in this cascade. Phosphorylation of PKB at Thr308 and Ser473 is associated with its full activation, whereas phosphorylation of GSK-3 (Ser21 of GSK-3 α and Ser9 of GSK-3 β) results in inactivation of GSK-3. Insulin-stimulated PKB phosphorylation was markedly higher in liver extracts of GSK-3 α KO mice compared

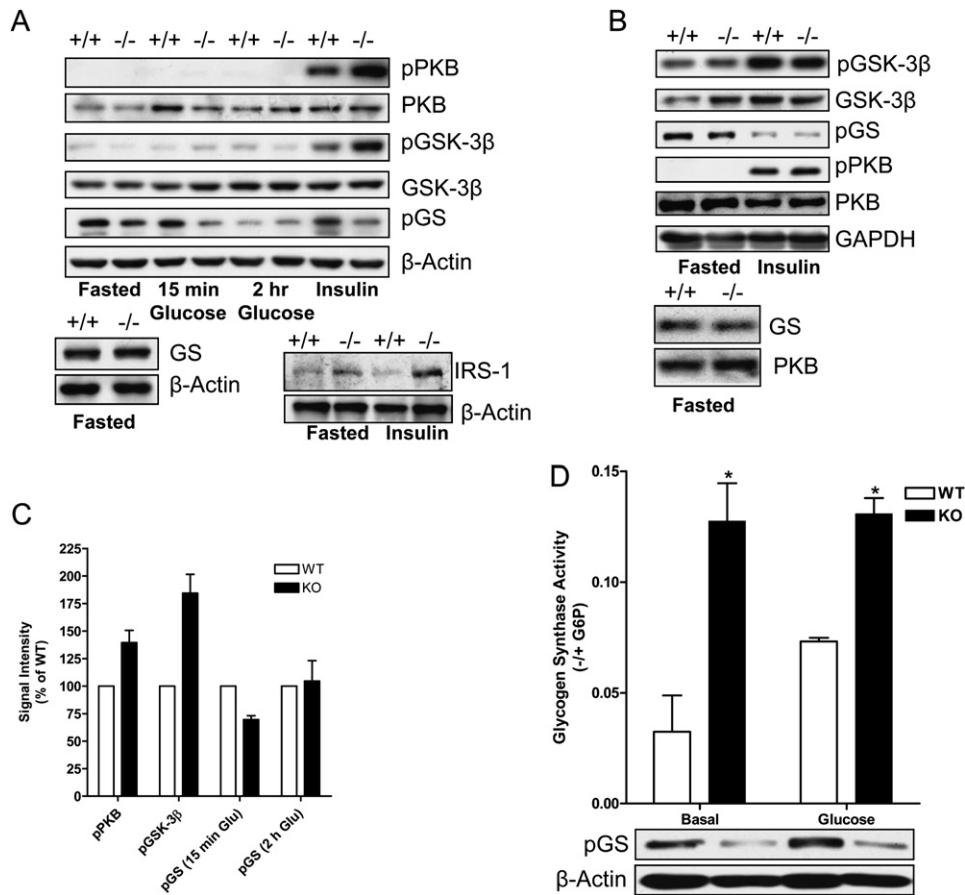


Figure 3. Effect of GSK-3 α Loss on the Insulin Signaling Pathway

(A and B) Liver (A) and muscle (B) from 8-week-old GSK-3 α KO (-/-) and WT (+/+) littermates was extracted at the indicated times after i.p. insulin or glucose injection, and 20 μ g of the protein lysate was resolved by SDS-PAGE. Proteins were detected by immunoblotting with antibodies against phospho-PKB, PKB, phospho-GSK-3 β , GSK-3 β , phospho-GS, GS (lower left in [A] and [B]), and IRS-1 (lower right in [A]). β -actin or GAPDH was used as a loading control. Blots are representative of three separate experiments.

(C) Quantification of immunoreactivity of insulin-stimulated phospho-PKB and phospho-GSK-3 β and glucose-stimulated phospho-GS (15 min and 2 hr) from WT and GSK-3 α KO liver tissue. Data are presented as a bar graph showing signal intensity as percentage of WT signal. $n \geq 3$ independent experiments.

(D) Primary hepatocytes were isolated as described in [Experimental Procedures](#) and pretreated with or without 25 mM glucose for 30 min. GS activity was determined by assaying incorporation of glucose from UDP-[6- 3 H]D-glucose into glycogen and is expressed as a ratio of activity in the absence of G6P to activity in the presence of G6P. Lower panel shows a representative phospho-GS immunoblot of assayed lysates. β -actin was used as a loading control. $n = 3$ experiments carried out in duplicate; * $p < 0.01$ versus the respective fasted control.

to WT mice (Figure 3A). Consistent with this finding, insulin-stimulated phosphorylation of GSK-3 β was higher in extracts from livers of GSK-3 α KO mice than in WT liver extracts. However, in contrast to in the liver, levels of insulin-stimulated phosphorylation of PKB and GSK-3 β were similar in skeletal muscle from both WT and GSK-3 α KO mice (Figure 3B).

Liver GS is controlled by the allosteric activator glucose-6-phosphate (G6P) in addition to phosphorylation. Using a phosphospecific antibody to the GSK-3 site Ser641, GS was found to be less phosphorylated, and hence more active, in liver extracts from GSK-3 α KO compared to WT control animals (Figure 3A). Acute (15 min) administration of glucose led to dephosphorylation of GS in livers from GSK-3 α KO mice, whereas no

dephosphorylation of GS was observed in control animals (Figure 3A). However, following 2 hr glucose administration, the phosphorylation status of GS was comparable in liver extracts from GSK-3 α KO and WT animals. Expression of insulin receptor substrate 1 (IRS-1) was markedly higher in GSK-3 α KO compared to WT liver samples (Figure 3A, lower right panel). In agreement with the phosphorylation and glucose transport data, analysis of skeletal muscle revealed negligible differences in insulin-stimulated dephosphorylation of GS (Figure 3B). Analysis of isolated primary hepatocytes demonstrated significantly higher GS activity in unstimulated GSK-3 α KO hepatocytes compared to WT cells. Although a 30 min glucose treatment resulted in elevated GS activity in WT hepatocytes, glucose-stimulated GSK-3 α KO hepatic

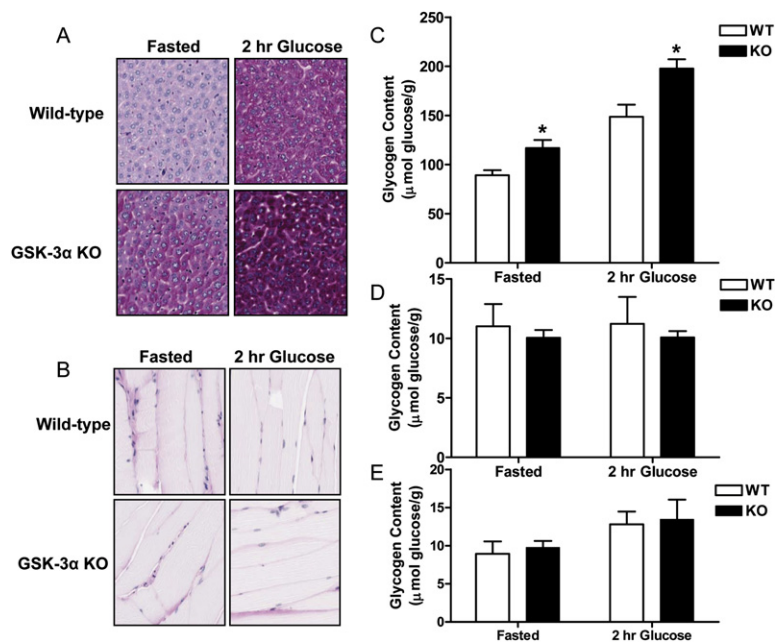


Figure 4. Glycogen Deposition in Liver, Muscle, and Epididymal Fat of GSK-3 α KO and WT Mice

(A and B) Periodic acid Schiff (PAS) staining of liver (A) and muscle (B) of 8-week-old GSK-3 α KO animals and WT littermate controls following fasting or a 2 hr administration of 2 mg/g glucose by i.p. injection. Images are representative of four separate animals.

(C–E) Glycogen content was measured in liver (C), muscle (D), and epididymal fat (E) from 8-week-old GSK-3 α KO (black bars) and WT (white bars) littermates following fasting or a 2 hr i.p. injection of 2 mg/g glucose. Tissues were extracted and acid hydrolyzed, and glycosyl units were assayed using a glucose reagent hexokinase method (Amresco) as described in *Experimental Procedures*. Glycogen content is expressed as $\mu\text{mol glucose/g}$ tissue. $n = 8$ animals; * $p < 0.05$ versus WT for fasted; * $p < 0.001$ versus WT for 2 hr glucose.

GS activity remained comparable to that observed under basal conditions (Figure 3D). Analysis of GS phosphorylation from isolated primary hepatocytes was consistent with these findings (Figure 3D). Expression analysis of gluconeogenic genes demonstrated no significant alteration in phosphoenolpyruvate carboxykinase (PEPCK), phosphofructokinase (PFK), and G6Pase mRNA expression between GSK-3 α KO and WT livers under fasted conditions or following a 2 hr administration of insulin (Figure S3). However, glucokinase (GCK) mRNA expression was increased under fasted conditions in GSK-3 α KO samples compared to WT (Figure S3). This difference was not observed in the presence of insulin.

Increased Glycogen Deposition in GSK-3 α KO Liver

A major contribution to the pathophysiology of diabetes is impaired storage and utilization of glucose (Cline et al., 1994; Shulman et al., 1990a). Periodic acid Schiff (PAS) staining was used to detect glycogen in sections of paraffin-embedded liver from GSK-3 α KO and WT mice. Fasted WT liver showed minimal glycogen content (Figure 4A), whereas liver sections from fasted GSK-3 α KO animals exhibited significantly elevated glycogen (Figure 4A). Glycogen levels 2 hr after glucose administration were substantially elevated in GSK-3 α KO mouse liver compared to WT. In contrast, no differences were observed in muscle glycogen content between fasted or glucose-injected WT and GSK-3 α KO animals (Figure 4B). Quantitative enzymatic analysis of glycogen was consistent with the PAS staining such that fasted and glucose-stimulated liver glycogen was enhanced in GSK-3 α KO animals (Figure 4C) with no significant difference in muscle (Figure 4D) or epididymal fat pad (Figure 4E) glycogen.

Both WT and GSK-3 α KO hepatic glycogen levels were significantly elevated following feeding; however, no difference was observed between the two animal groups (Figure S4).

To determine whether the tissue difference in glycogen levels related to compartmentalization of GSK-3 isoforms, we isolated the glycogen pellet from liver and muscle of WT and KO animals (Figure S5A). Although the ratio of GSK-3 α to GSK-3 β associated with the glycogen pellet was comparable between liver and muscle in WT animals, the ratio of GSK-3 α to GSK-3 β was significantly higher in the supernatant of WT muscle than in WT liver (Figure S5B). Additionally, PP1 association with the glycogen pellet from liver and muscle was comparable between the two animal groups (Figure S5A). To assess whether hepatic GS regulation was GSK-3 α -specific, we compared the phosphorylation of GS in liver from WT and GSK-3 α KO animals and from animals with conditional deletion of GSK-3 β in the liver (S.P. and J.R.W., unpublished data). GS phosphorylation was significantly lower in liver from GSK-3 α KO animals compared to WT controls, whereas phosphorylation of GS in GSK-3 β KO liver samples was comparable to that observed in WT animals (Figure S5C).

DISCUSSION

Acute and chronic inhibition of GSK-3 by either insulin or cell-permeable chemical inhibitors can result in activation of GS activity and glycogen deposition in a variety of cells and tissues (see, e.g., Coghlan et al., 2000; Eldar-Finkelman et al., 1996; MacAulay et al., 2003; Orena et al., 2000). GSK-3 expression and activity are elevated in diabetic rodents and humans, with consequential

suppression of GS activity (Damsbo et al., 1991; Henry et al., 1996) and severely impaired glycogen deposition (Shulman et al., 1990b). The majority of the prior studies have addressed the importance of GSK-3 for glucose metabolism via either overexpression of GSK-3 mutants or application of pharmacological inhibitors that block both GSK-3 isoforms. Here, we present genetic evidence supporting an essential role for GSK-3 α in glucose homeostasis and demonstrate unique, tissue-specific physiological functions of GSK-3 α and GSK-3 β .

Our finding that global loss of GSK-3 α results in improved glucose tolerance and insulin sensitivity in mice is supported by reports demonstrating the beneficial effects of acute GSK-3 inhibition in mouse models of diabetes and obesity (Cline et al., 2002; Henriksen et al., 2003; Kaidanovich-Beilin and Eldar-Finkelman, 2006). The enhanced insulin sensitivity observed in GSK-3 α KO mice may be explained by the reduction in total fat mass and increase in total lean mass. Circulating leptin levels are directly proportional to total body fat mass (Friedman and Halaas, 1998); hence, the alteration in body composition is consistent with our finding that plasma leptin levels were significantly reduced in fed GSK-3 α KO mice compared to WT littermates.

The most striking physiological phenotype of the GSK-3 α KO mice is significant enhancement of fasted and glucose-stimulated hepatic glycogen deposition. Cline et al. (2002) demonstrated increased liver glycogen deposition in Zucker diabetic fatty rats treated with GSK-3 inhibitors, with little effect on skeletal muscle glycogen levels. Interestingly, overexpression of GSK-3 β in muscle results in reduced muscle glycogen deposition accompanied by a compensatory increase in liver glycogen levels (Pearce et al., 2004). Liver glycogen accumulation has also been observed in the absence of muscle glycogen in mice lacking muscle GS (Pederson et al., 2005). These latter studies suggest that some level of compensatory tissue crosstalk exists with respect to the regulation of glycogen deposition. The fact that there were no differences in GS activity or glycogen deposition in muscle suggests that GSK-3 α may have a minimal role in the regulation of glycogen synthesis in this tissue. McManus et al. (2005) used a knockin approach to express constitutively active GSK-3 α and β (GSK-3 $\alpha^{21A/21A}$ /GSK-3 $\beta^{9A/9A}$). They reported that although insulin failed to stimulate an increase in GS activity in GSK-3 $\beta^{9A/9A}$ animals, an activation of GS was observed in response to insulin in GSK-3 $\alpha^{21A/21A}$ animals. The authors concluded that GSK-3 β , rather than GSK-3 α , is the primary muscle GS kinase.

GSK-3 α KO liver extracts exhibited enhanced insulin-stimulated PKB and GSK-3 β phosphorylation, whereas in muscle, phosphorylation of these proteins was comparable between WT and KO animals. The reason behind this enhanced insulin signaling in the liver but not the muscle is unclear. A possible explanation for the enhanced liver PKB and GSK-3 β phosphorylation is that IRS-1 serine phosphorylation is decreased in GSK-3 α KO liver. GSK-3 has previously been shown to catalyze serine phosphorylation

of IRS-1, interfering with receptor-mediated tyrosine phosphorylation by the insulin receptor, effectively attenuating insulin receptor signaling through negative feedback (Liberman and Eldar-Finkelman, 2005). Loss of GSK-3 α in the liver may result in reduced IRS-1 serine phosphorylation and hence augment insulin signaling. Hepatic IRS-1 protein levels were increased markedly in extracts from GSK-3 α KO animals. Previous reports have shown that acute insulin exposure results in stabilization of IRS-1 (Ruiz-Alcaraz et al., 2005). It has also been reported that serine/threonine phosphorylation of IRS-1 promotes its degradation (White, 2002). This mechanism is further supported by the finding that in *ob/ob* mice, in which GSK-3 activity has been reported to be elevated (Eldar-Finkelman et al., 1999), IRS-1 expression is reduced (Kerouz et al., 1997). Furthermore, it has recently been reported that knockdown of GSK-3 α in muscle cells from diabetic patients results in increased IRS-1 expression (Ciaraldi et al., 2007).

Our finding that GSK-3 α KO mice are viable contrasts with the embryonic lethality of GSK-3 β KO mice (Hoefflich et al., 2000) and indicates functional divergence between the isoforms. The importance of GSK-3 α has been overlooked in many areas of research to date due to the majority of studies focusing on GSK-3 β . However, the current findings demonstrate that GSK-3 α is a key regulator of hepatic glucose metabolism and indicate that GSK-3 α and GSK-3 β exhibit divergent physiological roles in muscle and liver tissue. A major concern in utilizing GSK-3 as a drug target is its role in the Wnt signaling pathway, where inhibition might lead to stabilization of the proto-oncogene β -catenin. However, GSK-3 α KO mice showed no increased propensity for tumorigenesis (data not shown). Furthermore, recent studies have demonstrated that complete loss of GSK-3 (i.e., GSK-3 $\alpha^{-/-}\beta^{-/-}$) in embryonic stem (ES) cells is required before β -catenin levels are significantly dysregulated (Doble et al., 2007). Together, these findings should mitigate previous concerns that inhibition of GSK-3 could be oncogenic and provide new incentive for examination of GSK-3 as a therapeutic target for type II diabetes, recognizing there are significant species differences between rodents and humans in tissue glycogen storage (Carey et al., 2003).

EXPERIMENTAL PROCEDURES

Conditional Knockout Mouse Generation

A targeting vector was employed that upon proper homologous recombination replaced exon 2 of the GSK-3 α gene with a conditional variant (LoxP-flanked). The "arms" of homology were obtained by PCR amplification of genomic DNA flanking exon 2 of the GSK-3 α gene with the proofreading polymerase Platinum Pfx (Invitrogen). The template DNA for PCR was obtained from a lambda phage clone isolated by Southern blotting from a library containing genomic DNA from the mouse strain 129/Ola. PCR products were sequence validated. The targeting vector (50 μ g) was linearized with NdeI, purified, and electroporated into 8×10^6 cells of the hybrid 129/B6 ES cell line designated G4 (George et al., 2007) with a Bio-Rad Gene Pulser II (250V, 500 μ F). After selection in G418-containing medium (250 μ g/ml), resistant clones were screened by PCR and Southern blotting (Figure 1B). One of the validated ES cell clones (+3.20*) was used in

aggregations with tetraploid embryos to generate mice derived entirely from the ES cells, as has been previously reported for other hybrid ES cell lines (Li et al., 2005). The genotype of the eight resulting mice was confirmed by PCR analysis.

Male GSK-3 α KO mice and WT littermate controls were housed five per cage with a light/dark cycle of 12 hr in the Princess Margaret Hospital animal facility, with free access to food and water except where noted. For assessment of fat and lean mass, a mouse whole-body magnetic resonance analyzer (Echo Medical Systems) was used.

Glucose and Insulin Tolerance Tests

Glucose tolerance tests were carried out following overnight fast (16–18 hr). Mice were administered 2 mg/g glucose by i.p. injection, and blood glucose was assayed from the tail vein using a OneTouch Ultra-Smart Blood Glucose Monitoring System (LifeScan) at the indicated times. For insulin tolerance testing, animals were fasted for 5 hr prior to an i.p. injection of 1 mU/g insulin.

Plasma Insulin, Adiponectin, Leptin, and Triglyceride Assays

Blood was collected from the tail vein of random-fed mice following an overnight fast alone or after i.p. glucose administration as stated in the figure legends. Plasma was assayed for insulin, adiponectin, and leptin using a rat/mouse insulin ELISA kit, adiponectin ELISA kit, and mouse leptin ELISA kit, respectively (Linco Research). Plasma triglycerides were determined using a Wako L-Type Triglyceride-H kit (Wako Chemicals USA, Inc.).

Preparation of Tissue Lysates and Cytosolic

β -Catenin Isolation

Mice were fasted overnight and treated with 150 mU/g insulin for 10 min or 2 mg/g glucose for either 15 or 120 min by i.p. injection. Tissues were extracted in lysis buffer (150 mM NaCl, 1% NP-40, 0.5% DOC, 0.1% SDS, 1 mM EDTA, 50 mM Tris [pH 8.0], 10 mM sodium fluoride, 1 mM sodium orthovanadate, 10 mM β -glycerophosphate, and one protease inhibitor cocktail tablet/50 ml). Lysates were centrifuged at 16,000 \times g, 4°C for 15 min, and protein concentration was determined by Lowry assay (Lowry et al., 1951).

For cytoplasmic β -catenin isolation, tissue extracts from fasted mice were lysed in hypotonic lysis buffer (50 mM Tris [pH 7.4], 1 mM EDTA, 25 mM sodium fluoride, 1 mM sodium orthovanadate, 5 mM β -glycerophosphate, and protease inhibitors). Lysates were centrifuged at 300,000 \times g, 4°C for 30 min, and the supernatant was used as the source for cytosolic β -catenin.

Immunoblotting

Twenty micrograms of protein was resolved by SDS-PAGE and immunoblotted with antibodies against GSK-3 α/β (1:10,000, BioSource), phospho-GSK-3 β (1:1,000, Cell Signaling), β -catenin (1:1,000, BD Transduction Laboratories), PKB (1:1,000, Cell Signaling), phospho-PKB Ser473 (1:1,000, Cell Signaling), GS (GYS1, 1:1,000, Chemicon), GS (GYS2, 1:1,000, gift from J. Guinovart, University of Barcelona), phospho-GS (1:1,000, Cell Signaling), IRS-1 (1 μ g/ml, Upstate), PP1 (1:1,000, BD Transduction Laboratories), β -actin (1:20,000, Abcam), GAPDH (1:100,000, Abcam), GLUT1 (1:1,000, Chemicon), GLUT4 (1:1,000, Chemicon), GLUT2 (1:1,000, Chemicon), and caveolin-1 (1:500, Abcam) overnight at 4°C. Washed membranes were incubated with species-appropriate HRP-linked secondary antibodies (1:10,000), and visualization was performed using ECL reagent exposure to Kodak film. Densitometry was performed using an Alpha Innotech FluorChem HD2.

Primary Hepatocyte Isolation and Culture

Eight-week-old GSK-3 α KO and WT littermate control animals were anesthetized with isoflurane/oxygen. Hepatocytes were then isolated by retrograde, nonrecirculating in situ collagenase liver perfusion. In brief: livers were perfused with liver perfusion medium (pH 7.4, Invitrogen) followed by liver digest medium (pH 7.4, Invitrogen). The digested liver was removed and washed in chilled hepatocyte wash medium

(Invitrogen). Viable cells were harvested by Percoll (Sigma) gradient. The final pellet was resuspended in Williams' E medium containing 200 nM L-glutamine, 5% FBS, 1 μ g/ml insulin, 100 units/ml penicillin, and 100 μ g/ml streptomycin. Cell viability was greater than 90%. Hepatocytes were plated at 300,000 cells per well of six-well plates. Hepatocytes were allowed to recover and attach for 4 hr before replacement of the medium with serum-free α MEM overnight. Prior to lysis (50 mM Tris [pH 7.4], 0.27 M sucrose, 1 mM sodium orthovanadate [pH 10], 1 mM EDTA, 1 mM EGTA, 10 mM sodium β -glycerophosphate, 50 mM sodium fluoride, 5 mM sodium pyrophosphate, 1% (w/v) Triton X-100, 0.1% (v/v) 2-mercaptoethanol, and protease inhibitor cocktail), glucose (25 mM) was added for 30 min, and cells were washed three times in ice-cold saline (150 mM), scraped, and homogenized with a syringe needle prior to centrifugation.

Glycogen Synthase Activity Assay

GS activity was assayed as described previously (MacAulay et al., 2005). Assay buffer (67 mM Tris [pH 7.5], 5 mM DTT, 89 mM UDP-glucose, 6.7 mM EDTA, 13 mg/ml glycogen, and 1 μ Ci/assay UDP-[6-³H]D-glucose) was added to 45 μ l of lysate in the presence or absence of 20 mM G6P. After incubation at 37°C for 30 min, the reaction was stopped by spotting onto 31ETCHR Whatman filter paper (Whatman International Ltd.) and washed three times in 66% ethanol for 20 min. Finally, filters were washed in acetone and air dried before incorporation of glucose from UDP-[6-³H]D-glucose (GE Healthcare) into glycogen was counted by liquid scintillation. GS activity was expressed as a ratio of activity in the absence of G6P to activity in the presence of G6P.

Periodic Acid Schiff Staining

Liver and muscle from mice either fasted overnight or fasted overnight and then given an i.p. injection of 2 mg/g glucose for 2 hr were extracted and fixed in 10% neutral buffered formalin overnight at 4°C. Tissues were sectioned and subjected to PAS staining prior to imaging (Amalfitano et al., 1999).

Glycogen Determination

Fifty milligrams of gastrocnemius, 20 mg of liver, or 50 mg of epididymal fat from mice fed as normal, fasted overnight, or fasted overnight and then given a 2 hr i.p. injection of 2 mg/g glucose was acid hydrolyzed in 2 M HCl at 95°C for 2 hr. Following neutralization in 2 M NaOH, glycosyl units were assayed using a glucose reagent hexokinase method (Amresco) as described previously (Bondar and Mead, 1974).

Statistical Analysis

For multiple comparisons, analysis was performed using either two-way analysis of variance (ANOVA) followed by a Bonferroni post hoc test or unpaired Student's t test. Data analysis was performed using GraphPad Prism software, and differences were considered statistically significant at $p < 0.05$ unless otherwise stated.

Supplemental Data

Supplemental Data include Supplemental Experimental Procedures, Supplemental References, and five figures and can be found with this article online at <http://www.cellmetabolism.org/cgi/content/full/6/4/329/DC1/>.

ACKNOWLEDGMENTS

This work was supported by postdoctoral fellowship awards from the Banting and Best Diabetes Centre (K.M.) and the Canadian Institutes of Health Research (B.W.D. and S.P.). Operating support was provided by the Canadian Institutes of Health Research (to J.R.W.). K.M. designed and performed the experiments and drafted the manuscript. B.W.D. generated and initially characterized the KO mice and participated in data analysis. S.P. generated the GSK-3 β hepatocyte-specific KO mice and provided technical support and manuscript revision. T.H. provided technical assistance and manuscript revision. E.M.S.

performed the primary hepatocyte isolation. D.J.D. provided technical facilities and manuscript critique. A.N. provided the hybrid B6/129 G4 mouse ES cell line and advice. J.R.W. conceived the studies and participated in experimental design and manuscript revision.

Received: April 12, 2007

Revised: July 14, 2007

Accepted: August 24, 2007

Published: October 2, 2007

REFERENCES

- Amalfitano, A., McVie-Wylie, A.J., Hu, H., Dawson, T.L., Raben, N., Plotz, P., and Chen, Y.T. (1999). Systemic correction of the muscle disorder glycogen storage disease type II after hepatic targeting of a modified adenovirus vector encoding human acid-alpha-glucosidase. *Proc. Natl. Acad. Sci. USA* 96, 8861–8866.
- Bondar, R.J., and Mead, D.C. (1974). Evaluation of glucose-6-phosphate dehydrogenase from *Leuconostoc mesenteroides* in the hexokinase method for determining glucose in serum. *Clin. Chem.* 20, 586–590.
- Carey, P.E., Halliday, J., Snaar, J.E., Morris, P.G., and Taylor, R. (2003). Direct assessment of muscle glycogen storage after mixed meals in normal and type 2 diabetic subjects. *Am. J. Physiol. Endocrinol. Metab.* 284, E688–E694.
- Ciaraldi, T.P., Nikoulina, S.E., Bandukwala, R.A., Carter, L., and Henry, R.R. (2007). Role of glycogen synthase kinase-3{alpha} in insulin action in cultured human skeletal muscle cells. *Endocrinology* 148, 4393–4399.
- Cline, G.W., Rothman, D.L., Magnusson, I., Katz, L.D., and Shulman, G.I. (1994). ¹³C-nuclear magnetic resonance spectroscopy studies of hepatic glucose metabolism in normal subjects and subjects with insulin-dependent diabetes mellitus. *J. Clin. Invest.* 94, 2369–2376.
- Cline, G.W., Johnson, K., Regittnig, W., Perret, P., Tozzo, E., Xiao, L., Damico, C., and Shulman, G.I. (2002). Effects of a novel glycogen synthase kinase-3 inhibitor on insulin-stimulated glucose metabolism in Zucker diabetic fatty (fa/fa) rats. *Diabetes* 51, 2903–2910.
- Coghlan, M.P., Culbert, A.A., Cross, D.A., Corcoran, S.L., Yates, J.W., Pearce, N.J., Rausch, O.L., Murphy, G.J., Carter, P.S., Roxbee Cox, L., et al. (2000). Selective small molecule inhibitors of glycogen synthase kinase-3 modulate glycogen metabolism and gene transcription. *Chem. Biol.* 7, 793–803.
- Damsbo, P., Vaag, A., Hother-Nielsen, O., and Beck-Nielsen, H. (1991). Reduced glycogen synthase activity in skeletal muscle from obese patients with and without type 2 (non-insulin-dependent) diabetes mellitus. *Diabetologia* 34, 239–245.
- Doble, B.W., Patel, S., Wood, G.A., Kockeritz, L.K., and Woodgett, J.R. (2007). Functional redundancy of GSK-3alpha and GSK-3beta in Wnt/beta-catenin signaling shown by using an allelic series of embryonic stem cell lines. *Dev. Cell* 12, 957–971.
- Dokken, B.B., Sloniger, J.A., and Henriksen, E.J. (2005). Acute selective glycogen synthase kinase-3 inhibition enhances insulin signaling in prediabetic insulin-resistant rat skeletal muscle. *Am. J. Physiol. Endocrinol. Metab.* 288, E1188–E1194.
- Eldar-Finkelman, H., Argast, G.M., Foord, O., Fischer, E.H., and Krebs, E.G. (1996). Expression and characterization of glycogen synthase kinase-3 mutants and their effect on glycogen synthase activity in intact cells. *Proc. Natl. Acad. Sci. USA* 93, 10228–10233.
- Eldar-Finkelman, H., Schreyer, S.A., Shinohara, M.M., LeBoeuf, R.C., and Krebs, E.G. (1999). Increased glycogen synthase kinase-3 activity in diabetes- and obesity-prone C57BL/6J mice. *Diabetes* 48, 1662–1666.
- Embi, N., Rylatt, D.B., and Cohen, P. (1980). Glycogen synthase kinase-3 from rabbit skeletal muscle. Separation from cyclic-AMP-dependent protein kinase and phosphorylase kinase. *Eur. J. Biochem.* 107, 519–527.
- Frame, S., Cohen, P., and Biondi, R.M. (2001). A common phosphate binding site explains the unique substrate specificity of GSK3 and its inactivation by phosphorylation. *Mol. Cell* 7, 1321–1327.
- Friedman, J.M., and Halaas, J.L. (1998). Leptin and the regulation of body weight in mammals. *Nature* 395, 763–770.
- George, S.H., Gertsenstein, M., Vintersten, K., Korets-Smith, E., Murphy, J., Stevens, M.E., Haigh, J.J., and Nagy, A. (2007). Developmental and adult phenotyping directly from mutant embryonic stem cells. *Proc. Natl. Acad. Sci. USA* 104, 4455–4460.
- Henriksen, E.J., Kinnick, T.R., Teachey, M.K., O'Keefe, M.P., Ring, D., Johnson, K.W., and Harrison, S.D. (2003). Modulation of muscle insulin resistance by selective inhibition of GSK-3 in Zucker diabetic fatty rats. *Am. J. Physiol. Endocrinol. Metab.* 284, E892–E900.
- Henry, R.R., Ciaraldi, T.P., Abrams-Carter, L., Mudaliar, S., Park, K.S., and Nikoulina, S.E. (1996). Glycogen synthase activity is reduced in cultured skeletal muscle cells of non-insulin-dependent diabetes mellitus subjects. Biochemical and molecular mechanisms. *J. Clin. Invest.* 98, 1231–1236.
- Hoeflich, K.P., Luo, J., Rubie, E.A., Tsao, M.S., Jin, O., and Woodgett, J.R. (2000). Requirement for glycogen synthase kinase-3beta in cell survival and NF-kappaB activation. *Nature* 406, 86–90.
- Kaidanovich, O., and Eldar-Finkelman, H. (2002). The role of glycogen synthase kinase-3 in insulin resistance and Type 2 diabetes. *Expert Opin. Ther. Targets* 6, 555–561.
- Kaidanovich-Beilin, O., and Eldar-Finkelman, H. (2006). Long-term treatment with novel glycogen synthase kinase-3 inhibitor improves glucose homeostasis in ob/ob mice: molecular characterization in liver and muscle. *J. Pharmacol. Exp. Ther.* 316, 17–24.
- Kerouz, N.J., Horsch, D., Pons, S., and Kahn, C.R. (1997). Differential regulation of insulin receptor substrates-1 and -2 (IRS-1 and IRS-2) and phosphatidylinositol 3-kinase isoforms in liver and muscle of the obese diabetic (ob/ob) mouse. *J. Clin. Invest.* 100, 3164–3172.
- Li, X., Yu, Y., Wei, W., Yong, J., Yang, J., You, J., Xiong, X., Qing, T., and Deng, H. (2005). Simple and efficient production of mice derived from embryonic stem cells aggregated with tetraploid embryos. *Mol. Reprod. Dev.* 71, 154–158.
- Lieberman, Z., and Eldar-Finkelman, H. (2005). Serine 332 phosphorylation of insulin receptor substrate-1 by glycogen synthase kinase-3 attenuates insulin signaling. *J. Biol. Chem.* 280, 4422–4428.
- Lowry, O.H., Rosebrough, N.J., Farr, A.L., and Randall, R.J. (1951). Protein measurement with the Folin phenol reagent. *J. Biol. Chem.* 193, 265–275.
- MacAulay, K., Hajdich, E., Blair, A.S., Coghlan, M.P., Smith, S.A., and Hundal, H.S. (2003). Use of lithium and SB-415286 to explore the role of glycogen synthase kinase-3 in the regulation of glucose transport and glycogen synthase. *Eur. J. Biochem.* 270, 3829–3838.
- MacAulay, K., Blair, A.S., Hajdich, E., Terashima, T., Baba, O., Sutherland, C., and Hundal, H.S. (2005). Constitutive activation of GSK3 down-regulates glycogen synthase abundance and glycogen deposition in rat skeletal muscle cells. *J. Biol. Chem.* 280, 9509–9518.
- McManus, E.J., Sakamoto, K., Armit, L.J., Ronaldson, L., Shpiro, N., Marquez, R., and Alessi, D.R. (2005). Role that phosphorylation of GSK3 plays in insulin and Wnt signalling defined by knockin analysis. *EMBO J.* 24, 1571–1583.
- Nikoulina, S.E., Ciaraldi, T.P., Mudaliar, S., Mohideen, P., Carter, L., and Henry, R.R. (2000). Potential role of glycogen synthase kinase-3 in skeletal muscle insulin resistance of type 2 diabetes. *Diabetes* 49, 263–271.
- Orena, S.J., Torchia, A.J., and Garofalo, R.S. (2000). Inhibition of glycogen-synthase kinase 3 stimulates glycogen synthase and glucose transport by distinct mechanisms in 3T3-L1 adipocytes. *J. Biol. Chem.* 275, 15765–15772.

Pearce, N.J., Arch, J.R., Clapham, J.C., Coghlan, M.P., Corcoran, S.L., Lister, C.A., Llano, A., Moore, G.B., Murphy, G.J., Smith, S.A., et al. (2004). Development of glucose intolerance in male transgenic mice overexpressing human glycogen synthase kinase-3 β on a muscle-specific promoter. *Metabolism* 53, 1322–1330.

Pederson, B.A., Schroeder, J.M., Parker, G.E., Smith, M.W., DePaoli-Roach, A.A., and Roach, P.J. (2005). Glucose metabolism in mice lacking muscle glycogen synthase. *Diabetes* 54, 3466–3473.

Roach, P.J. (2002). Glycogen and its metabolism. *Curr. Mol. Med.* 2, 101–120.

Ruiz-Alcaraz, A.J., Liu, H.K., Cuthbertson, D.J., McManus, E.J., Akhtar, S., Lipina, C., Morris, A.D., Petrie, J.R., Hundal, H.S., and Sutherland, C. (2005). A novel regulation of IRS1 (insulin receptor substrate-1) expression following short term insulin administration. *Biochem. J.* 392, 345–352.

Shulman, G.I., Cline, G., Schumann, W.C., Chandramouli, V., Kumaran, K., and Landau, B.R. (1990a). Quantitative comparison of pathways of hepatic glycogen repletion in fed and fasted humans. *Am. J. Physiol.* 259, E335–E341.

Shulman, G.I., Rothman, D.L., Jue, T., Stein, P., DeFronzo, R.A., and Shulman, R.G. (1990b). Quantitation of muscle glycogen synthesis in normal subjects and subjects with non-insulin-dependent diabetes by ¹³C nuclear magnetic resonance spectroscopy. *N. Engl. J. Med.* 322, 223–228.

White, M.F. (2002). IRS proteins and the common path to diabetes. *Am. J. Physiol. Endocrinol. Metab.* 283, E413–E422.

Woodgett, J.R. (1990). Molecular cloning and expression of glycogen synthase kinase-3/factor A. *EMBO J.* 9, 2431–2438.

Supplemental Data

Short Article

Glycogen Synthase Kinase 3 α -Specific Regulation

of Murine Hepatic Glycogen Metabolism

Katrina MacAulay, Bradley W. Doble, Satish Patel, Tanya Hansotia, Elaine M. Sinclair, Daniel J. Drucker, Andras Nagy, James R. Woodgett

Supplemental Experimental Procedures

Assessment of Food Intake

Mice were fasted overnight (16-18 h), weighed, and placed into individual cages containing pre-weighed rodent chow, with free access to water. Food was reweighed after 2, 4, 8 and 24 h and food intake expressed as gram food intake per gram body weight.

Total Membrane Extraction

Gastrocnemius muscle or liver was extracted following an overnight fast. Tissues were minced in homogenization buffer (20 mM NaHCO₃, 250 mM sucrose, 5 mM NaN₃, 1 mM EDTA and protease inhibitor cocktail) and homogenized using a Brinkman Polytron. Homogenates were centrifuged at 1,300 g for 10 min and the pellet re-suspended, homogenized and re-centrifuged at 1,300 g for 10 min. The resulting supernatant was pooled with the first supernatant. The supernatants were then centrifuged at 9,000 g for 10 min, the pellet re-suspended in homogenization buffer and re-centrifuged at 229,000 g for 90 min. The pellet, containing the total membranes, was re-suspended in homogenization buffer and protein concentration determined by Lowry assay.

Muscle Glucose Transport Assay

Animals were fasted overnight and anaesthetized by i.p. injection of 100-200 μ l/10 g avertin. Soleus and EDL muscles were extracted and incubated for 30 min at 30 °C in Krebs Ringer Bicarbonate (KRB) buffer (137 mM NaCl, 5 mM KCl, 1.2 mM MgSO₄, 1 mM NaH₂PO₄, 1 mM CaCl₂, 24 mM NaHCO₃ and 0.1% BSA) followed by 30 min at 30 °C in KRB buffer containing 8 mM glucose and 32 mM mannitol in the absence or presence of 2 mU/ml insulin. Muscles were washed for 10 min in KRB buffer containing 32 mM mannitol in the absence or presence of 2 mU/ml insulin. Transport was assayed by incubation in KRB buffer containing 8 mM 2-deoxy-[³H]-D-glucose (2.25 μ Ci/ml), 32 mM D-[¹⁴C]-mannitol (0.3 μ Ci/ml) and 2 mM pyruvate in the absence or presence of 2 mU/ml insulin for 20 min at 30 °C. Tissues were continuously gassed with 95 % O₂/5 % CO₂ throughout the experiment. Muscles were blotted on filter paper, weighed and lysed in 1 M NaOH for 1 h at 85 °C. ³H and ¹⁴C radioactivity was quantified using a Beckman LS 6500 scintillation counter. ¹⁴C mannitol counts provide a means to calculate extracellular ³H volume and enabled calculation of total 2-deoxy-[³H]-D-glucose transported into the muscle tissue.

Real-Time Quantitative RT-PCR

Eight week old GSK-3 α KO (filled bars) and WT (open bars) animals were either fasted overnight (16-18 h) or fasted for 5 h prior to a 2 h administration of insulin (1 mU/g) by i.p. injection. Livers were harvested, snap frozen and stored at -80 °C. Total RNA was isolated using TRIzol® reagent as per manufacturer's instructions (Invitrogen). First-strand cDNA was synthesized from total RNA using Superscript™ II Reverse Transcriptase Kit (Invitrogen) and hexamers. Real-time quantitative PCR analysis was performed using TaqMan Gene Expression Assays and TaqMan Universal PCR Master Mix (Applied Biosystems) using the ABI Prism 7900 Sequence Detection Systems according to the protocols provided by the manufacturer (Applied Biosystems). The relative mRNA transcript levels were calculated according to the $2^{-\Delta CT}$ method (Livak and Schmittgen, 2001), in which ΔCT represents the difference in threshold cycle values between target mRNA and the 18S internal control.

Glycogen Pellet Isolation

Animals were fed *ad libitum* prior to liver and muscle extraction. Tissues were lysed in 3 vol./g of ice cold 2 mM EDTA, pH 7.0, 2 mM EGTA, 250 mM sucrose, 0.1% (v/v) 2-mercaptoethanol, one 'Complete' protease inhibitor cocktail tablet/ 50 ml. Lysates were centrifuged (16,000 g, 4 °C for 15 min) and the resulting supernatant was centrifuged at 100,000 g, 4 °C for 90 min. The supernatant was retained and the pellet re-suspended in 1 vol. buffer A (50 mM Tris/HCl, pH 7.0, 0.1 mM EGTA, 5% (v/v) glycerol, 0.1% (v/v) 2-mercaptoethanol and protease inhibitor cocktail) plus 300 mM NaCl and re-centrifuged at 100,000 g, 4 °C for 90 min. The supernatant was discarded and the glycogen pellet was re-suspended in 0.5 vol. of buffer A as described (Browne et al., 2001) and protein concentration determined by Lowry assay.

Supplemental References

Browne, G. J., Delibegovic, M., Keppens, S., Stalmans, W., and Cohen, P. T. (2001). The level of the glycogen targeting regulatory subunit R5 of protein phosphatase 1 is decreased in the livers of insulin-dependent diabetic rats and starved rats. *Biochem J* 360, 449-459.

Livak, K. J., and Schmittgen, T. D. (2001). Analysis of relative gene expression data using real-time quantitative PCR and the $2^{-\Delta\Delta C(T)}$ Method. *Methods* 25, 402-408.

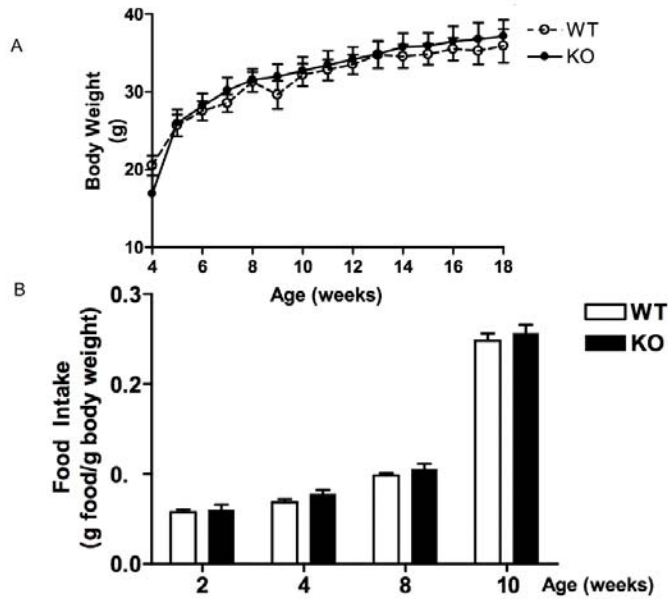


Figure S1. Body Mass and Food Intake of GSK-3 α KO Mice

(A) Body weight of male GSK-3 α KO (filled circles) and WT (open circles) littermate control mice was monitored weekly from ages 4 to 18 weeks. Values are the mean \pm SEM from 5 separate animals.

(B) GSK-3 α KO (filled bars) and WT (open bars) animals were fasted overnight (16-18 h), placed in individual cages and food intake monitored after 2, 4, 8 and 24 h. Data are expressed as gram food per gram body weight. Results are the means \pm SEM from at least 6 independent animals.

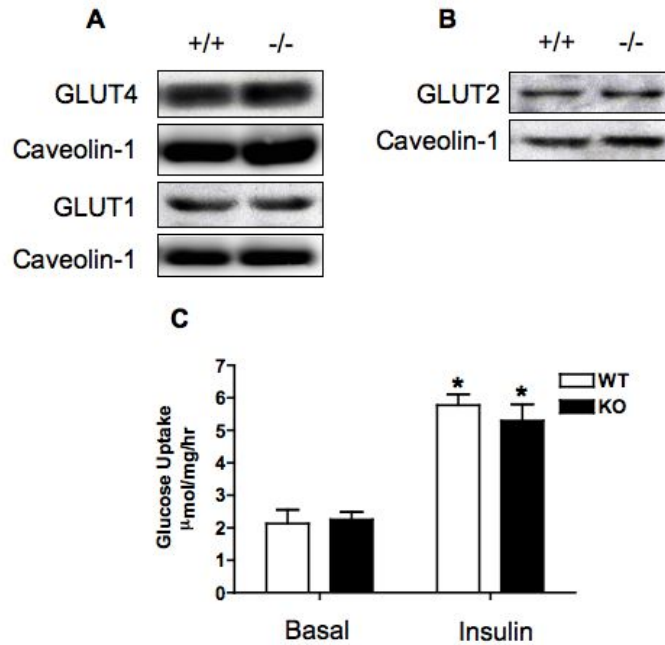


Figure S2. Glucose Transporter Expression and Activity in Muscle and Liver of GSK-3 α KO and WT Mice

(A and B) Muscle (A) and liver (B) was isolated from fasted animals and subjected to total membrane extraction as described in Experimental Procedures. 20 μ g total membrane lysate was resolved by SDS-PAGE and immunoblotted with antibodies against GLUT1, GLUT4 or GLUT2. Even loading was determined by immunoblotting with antibodies against caveolin-1. The blots are representative from three separate experiments.

(C) Soleus muscles were isolated from eight week old male GSK3 α KO (filled bars) and WT (open bars) littermate control animals and incubated with or without 2 mU of insulin per ml for 30 min. 2-deoxyglucose uptake was measured over a 20 min period as described in Experimental Procedures. Results are the means \pm SEM from at least 3 independent experiments. Asterisks signify statistically significant changes from the respective fasted control ($p < 0.001$).

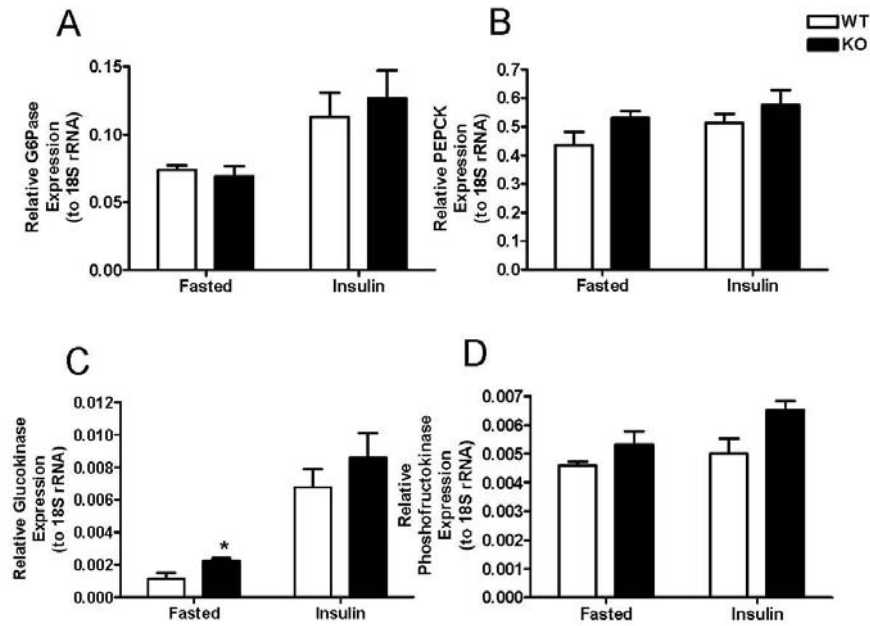


Figure S3. Gluconeogenic Gene Expression

Relative mRNA expression of G6Pase (A), PEPCCK (B), glucokinase (C), and phosphofruktokinase (D) in liver from 8 week old GSK-3 α KO (filled bars) and WT (open bars) littermate controls. Values are mean \pm SEM from 6 separate animals. Asterisks signify statistically significant changes from the respective WT control (p < 0.05).

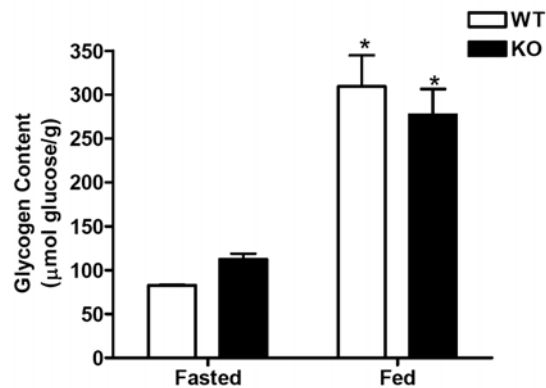


Figure S4. Glycogen Deposition in Liver of Fed Animals

Glycogen content was measured in liver from 8 week old GSK-3 α KO (filled bars) and WT (open bars) littermate control animals following overnight feeding. Tissues were extracted, acid-hydrolyzed and glycosyl units assayed using a glucose reagent hexokinase method (Amresco, Ohio) as described in Experimental Procedures. Glycogen content is expressed as μ mol glucose/g tissue. Values are mean \pm SEM from 3 separate animals. Asterisks signify statistically significant changes from the respective control (p < 0.001).

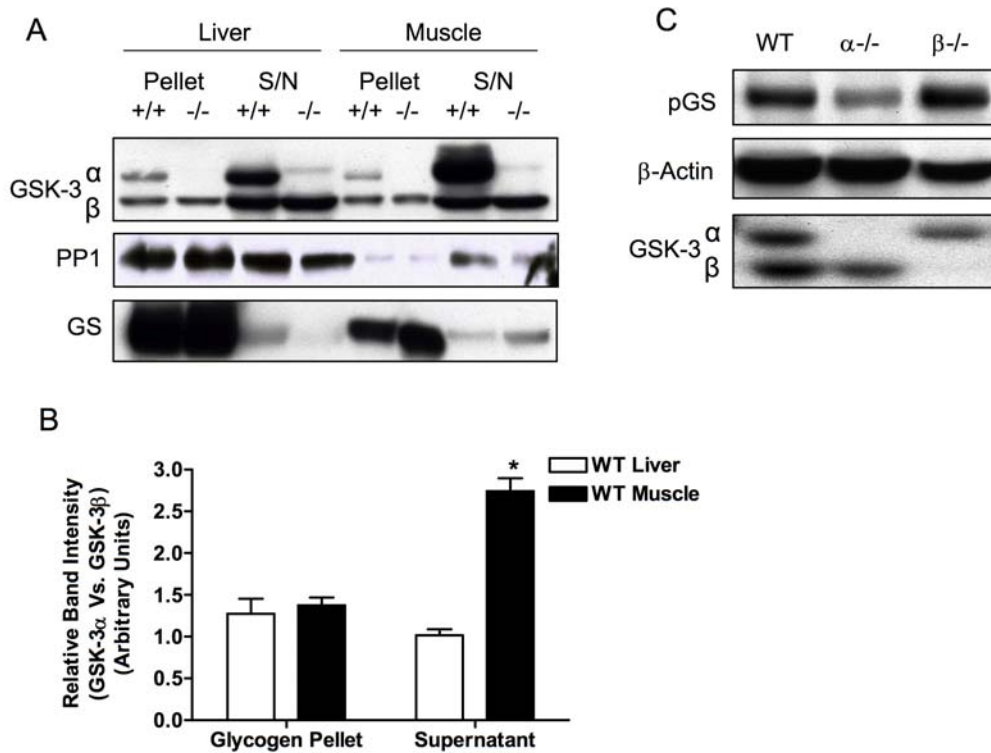


Figure S5. GSK-3α/β Association with the Glycogen Pellet

(A) Liver and muscle extracted from 8 week old GSK-3α KO (-/-) and WT (+/+) littermates following overnight feeding. Tissues were lysed and subjected to high-speed centrifugation. 25 μg protein of the resulting glycogen containing pellet (pellet) and supernatant (S/N) were resolved by SDS-PAGE and immunoblotted with antibodies against GSK-3α/β and PP1. Glycogen pellet isolation was determined by immunoblotting with antibodies against GS. Blots are representative from 3 separate experiments.

(B) Immunoreactive signals were quantified and data presented as a bar graph. Asterisks signify statistically significant changes ($p < 0.001$).

(C) Liver extracted from 8 week old GSK-3α KO (α-/-) and WT (WT) littermate control animals and animals with conditional liver GSK-3β KO (β-/-) following an overnight fast. 20 μg protein lysate was resolved by SDS-PAGE and proteins were detected by immunoblotting with antibodies against phospho-GS and GSK-3α/β. Even loading was determined using antibodies to β-actin. Blots are representative from 3 separate experiments.